Turing Patterns in CNNs—Part I: Once Over Lightly

Liviu Goraş, *Member, IEEE,* Leon O. Chua, *Fellow, IEEE,* and Domine M. W. Leenaerts, *Member, IEEE*

Abstract— **The aim of this three part tutorial is to focus the reader's attention to a new exciting behavior of a particular class of cellular neural networks (CNNs): Turing pattern formation in two-grid coupled CNNs. We first analyze the reduced Chua's circuit as the basic cell for the two-grid coupled CNNs capable of producing Turing patterns. We use a nonstandard normalization to derive a dimensionless state equation of the individual cell. Then, we present an intuitive explanation of Turing pattern formation mechanism for a 1-D two-grid coupled array in relation to the original mechanism proposed by Turing. Finally, we derive the first two conditions for Turing pattern formation, discuss the boundary conditions, and illustrate via an example on how the number of the equilibrium points of a CNN increases rapidly even though each isolated cell has only one equilibrium point. This study is continued in the next two parts of this tutorial where analytical derivations and various computer simulation results are presented as well.**

I. Introduction

WHAT are Patterns? The word *pattern*, widely used in various fields of scientific research, generally suggests meanings like configuration, form, specimen, and refers to time and/or space variable quantities.[1] In a certain sense, pattern is the opposite of uniformity or homogeneity. For instance, identical interacting elements (cells) placed in the nodes of a regular grid is said to give rise to a pattern only when they have unequal output states in the dc steady state.

Throughout this paper, the word "pattern" will denote the dc steady-state evolved through a differentiated dynamic behavior of identical elements identically coupled in a homogeneous (regular) spatial distribution. Thus, the case when all cells have identical output states will not be considered as representing a pattern.

It may seem somewhat surprising that in systems composed of identical and identically coupled elements (e.g., particles, mixtures of substances, biological cells, individuals of certain populations, and circuits in this paper) it is still possible for patterns to appear. Such phenomena, implying a "breakdown of symmetry" are currently being intensely studied in biology, physics, chemistry, ecology, and recently [1], [2] in electronics (Fig. 1). A typical example from physics is the Rayleigh-Bénard convection [3], [4], which denotes the phenomenon of circulating flow that takes place in the case of a fluid placed in a flat horizontal box uniformly heated and cooled at the bottom and the top, respectively. Autocatalytic chemical reactions coupled with molecular diffusion can generate patterns in biological, chemical, and biochemical systems following Alan Turing's celebrated model of morphogenesis[2] [5], [6]. In all cases, the shape and dimensions of the patterns depend, among other parameters, on the initial conditions, the boundary conditions, and the geometry and dimensions of the spatial domains.

A Glimpse Forward—The CNN: The recently introduced CNN circuit architecture [7], [8], is characterized by nonlinear, continuous-time, discrete-space dynamics. Its main feature consists of the fact that each cell[3] of the array is connected only to its neighboring ones[4] according to a template that is usually the same for all cells except for those in the boundary region. Sharing the best features of analog and digital circuits, including the ease of VLSI implementation, CNNs have been successfully used for various high speed parallel signal processing applications [9]. Under certain conditions, such arrays can produce patterns as well as many other spectacular dynamic phenomena, such as spiral, concentric, and scroll waves, etc. [2].

In the following, we begin the study of a particular family of CNNs having as cells Chua's circuits considered as resistive two-ports terminated in two capacitors and coupled by means of two rectangular resistive grids. We will show that these CNNs can produce patterns based on a mechanism similar to the reaction-diffusion phenomenon studied by Turing. The patterns obtained by this method will be called Turing patterns. In the 1-D case, the CNN consist of a chain of two-port cells having the corresponding ports linked by resistors. The 2-D case is sketched in Fig. 2 and may be viewed as a sandwich of cells between grids, each port of each cell being coupled to its four nearest adjacent corresponding neighbors through linear resistors. All cells are identical, and all resistors of each grid are equal to R_u and R_v, respectively.[5]

In this paper, we will refer to CNNs made of $M \times N$ cells arranged in a rectangular array of M rows and N columns. The 1-D case will correspond to $M = 1$.

Manuscript received December 5, 1994; revised March 14, 1995. This work was supported in part by the Office of Naval Research under Grant N00014-89-J-1402, by the National Science Foundation under Grant MIP-86–14000, and by the Dutch Foundation for Research (STW) under Project Number EEL44.3386. The work of L. Goraş was supported by the Fulbright Foundation. This paper was recommended by Guest Editor L. O. Chua.

The authors are with the Electronics Research Laboratory, University of California at Berkeley, Berkeley, CA 94720 USA.

IEEE Log Number 9414456.

[1] Pattern recognition should sound rather familiar to most readers.

[2] Morphogenesis is the part of embryology that studies the development of pattern and form as, for instance, animal coat patterns.

[3] Cells are identical.

[4] The r-neighborhood of a cell $C(i,j)$ is defined as $N_r(i,j) = \{C(k,l) | \max\{|k-i|, |l-j|\} \leq r\}$ for all admissible k and l in the array ($r \in \mathbf{N} \setminus \{0\}$).

[5] Generalization to nonhomogeneous arrays can also be made.

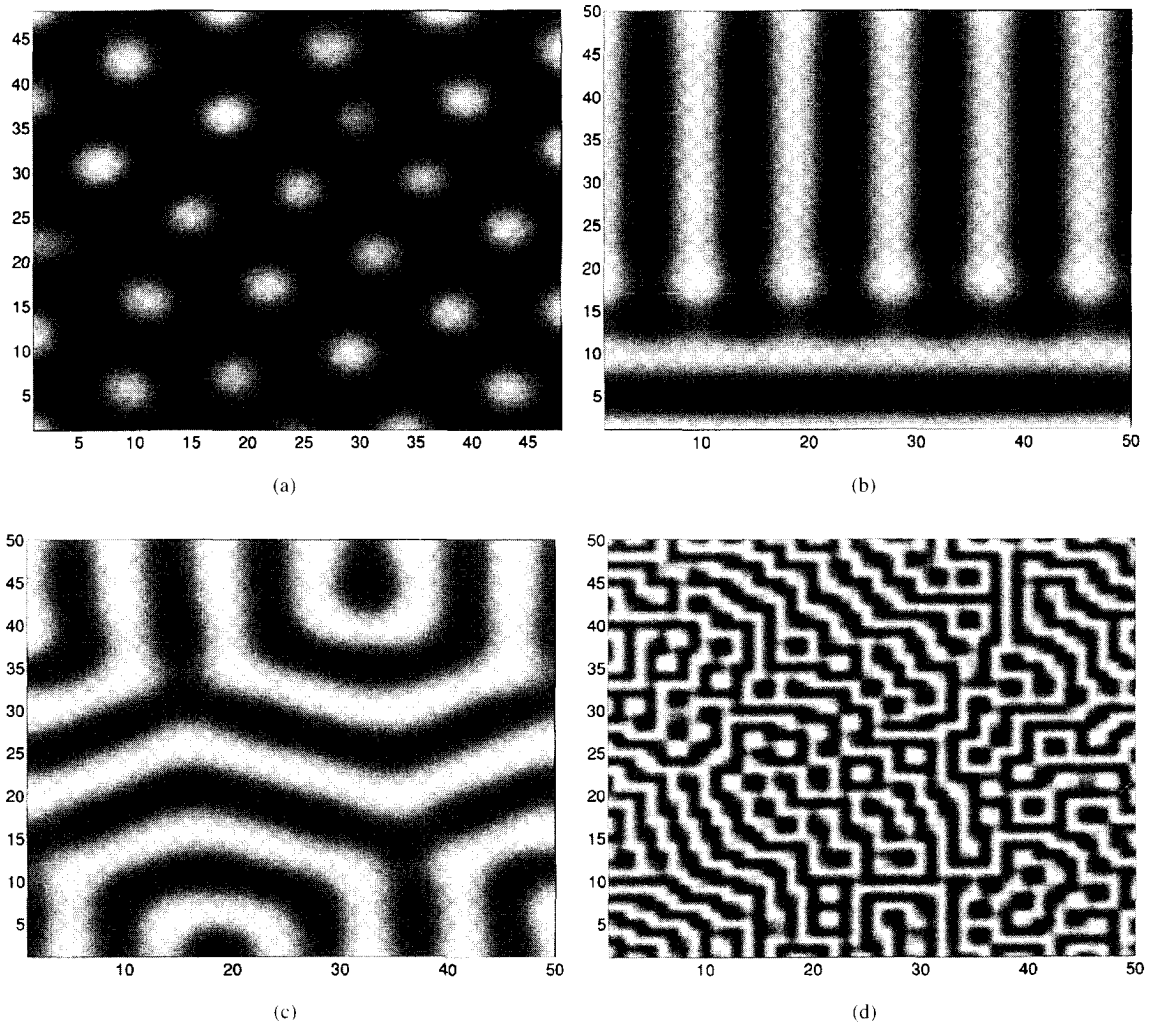

Fig. 1. Several voltage patterns obtained in a 50 × 50 cells two-grid coupled CNN (interpolation used for display).

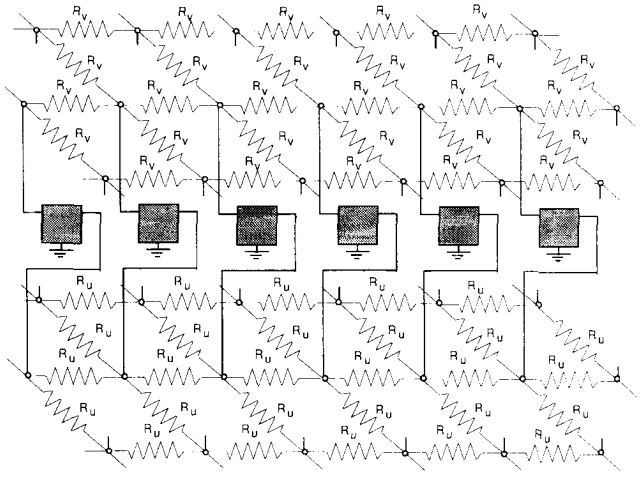

Fig. 2. Sketch of a two-grid coupled CNN. (For simplicity, only one row of cells is shown.)

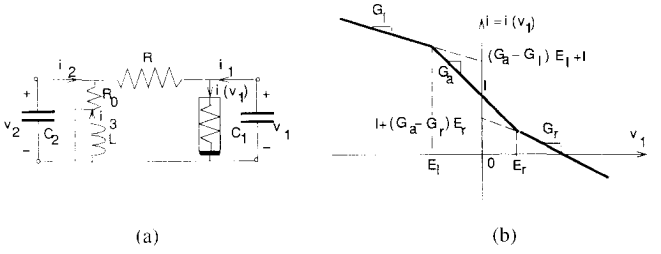

Fig. 3. (a) Chua's circuit. (b) v-i characteristic of Chua's diode.

II. The Cells

A. Equations and Normalizations

The Reduced Chua's Circuit: For Turing patterns to emerge, the cells of the two-grid coupled CNN should be at least of second order.[6] (It is known that even one-grid coupled CNNs based on the (third order) Chua's circuit may produce spatio-temporal chaos [10].) The reduced (second order) Chua's circuit, which will be used as a cell for the two-grid coupled CNN, is obtained from the original Chua's circuit by short circuiting the inductor as shown in Fig. 3, together with the piecewise-linear characteristic of the Chua's diode [1]. There are two reasons for making this simplification. *First*, most literature on Turing patterns used only second-order cells for the sake of simplicity. *Second*, our goal is to choose the simplest cell capable of producing Turing patterns. The

[6] Patterns are also possible from *first-order* cells, such as in the one-grid CNN [12], [13]. However, these patterns are not called Turing patterns.

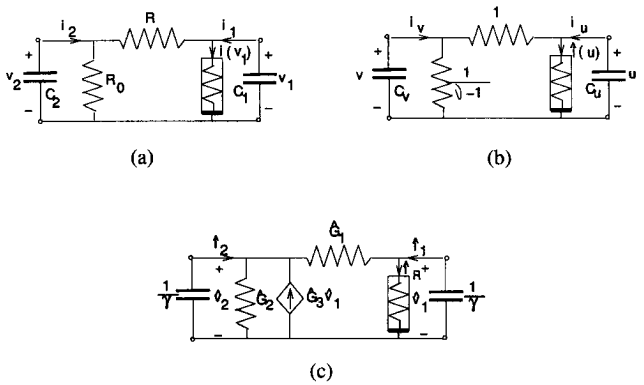

Fig. 4. The reduced Chua's circuit: (a) unnormalized; (b) normalized; (c) equivalent *reduced* Chua's circuit containing two identical positive capacitances.

reduced Chua's circuit is simpler not only because it has a lower-order state equation, but it contains only two kinds of two-terminal circuit elements, namely capacitors and resistors.

The reduced Chua's circuit will be regarded as a nonlinear resistive 2-port terminated by two linear capacitors as shown in Fig. 4(a). The resistive 2-port (consisting of Chua's diode and two linear resistors) is described by the general voltage-controlled constitutive relations

$$\begin{cases} i_1 = i_1(v_1, v_2) \\ i_2 = i_2(v_1, v_2). \end{cases} \tag{1}$$

Observe that, since it contains only 2-terminal resistors, the cell is reciprocal; i.e.

$$\frac{\partial i_1(v_1, v_2)}{\partial v_2} = \frac{\partial i_2(v_1, v_2)}{\partial v_1}. \tag{2}$$

The state equations describing each cell are given by

$$\begin{cases} C_1 \frac{dv_1}{dt} = -i_1(v_1, v_2) \\ C_2 \frac{dv_2}{dt} = -i_2(v_1, v_2) \end{cases} \tag{3}$$

and can be written explicitly as

$$\begin{cases} \frac{dv_1}{dt} = -\frac{G}{C_1} v_1 - \frac{1}{C_1} i(v_1) + \frac{G}{C_1} v_2 \\ \frac{dv_2}{dt} = \frac{G}{C_2} v_1 - \frac{(G+G_0)}{C_2} v_2 \end{cases} \tag{4}$$

where

$$i = i(v_1) = \begin{cases} G_l v_1 + (G_a - G_l) E_l + I, & \text{if } v_1 < E_l \\ G_a v_1 + I, & \text{if } E_l \le v_1 \le E_r \\ G_r v_1 + (G_a - G_r) E_r + I, & \text{if } v_1 > E_r \end{cases} \tag{5}$$

is the v-i characteristic of Chua's diode where the symbols are defined in Fig. 3(b).

Normalization: The standard normalization of the third-order Chua's circuit as well as that of the reduced Chua's circuit already used in the study of Turing patterns in [2] are presented in the Appendix. Even though such normalizations are sufficient for studying Turing patterns, they introduce some restrictions on the domains of existence as well as in the shape of the patterns. This is why in this paper we will use another normalization of the reduced Chua's circuit that will allow an extra degree of freedom when used in an array. Two particular features of our normalization procedure are the following: *first*, the Chua's diode characteristic is no longer considered symmetric and *second*, the normalizing capacitance is no longer equal to C_2 but an arbitrarily chosen positive value, C_0. Thus, both capacitors C_1 and C_2 (or their normalized values C_u and C_v) can be used to control the behavior of the cells and thus of the CNN.

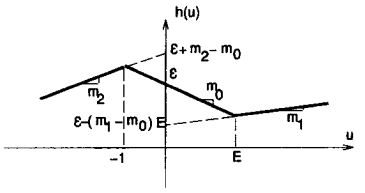

Fig. 5. $h(u)$ characteristic for the normalized reduced Chua's circuit.

Without loss of generality, we choose $G = \frac{1}{R}$, $C_0 = 1$, and $|E_l|$ as the normalizing values for resistors, capacitors, and voltages, respectively. The time scale will thus be normalized by the value RC_0. Multiplying both sides of (4) by $C_0/|E_l|G = 1/|E_l|G$ and introducing the notations[7]

$$\begin{aligned} u &= \frac{v_1}{|E_l|}, \quad v = \frac{v_2}{|E_l|}, \quad E = \frac{E_r}{|E_l|}, \\ C_u &= C_1, \quad C_v = C_2, \\ \nu &= 1 + \frac{G_0}{G}, \quad \gamma = \frac{1}{|C_1|} = \frac{1}{|C_u|}, \\ f(u,v) &= -\frac{|C_u|}{|E_l|GC_u} i_1(|E_l|u, |E_l|v) \\ &= -\frac{|C_u|}{C_u}(h(u) - v), \\ g(u,v) &= -\frac{|C_u|}{|E_l|GC_v} i_2(|E_l|u, |E_l|v) \\ &= \frac{|C_u|}{C_v}(u - \nu v) \end{aligned} \tag{6}$$

the new dimensionless equations for the reduced Chua's circuit now assume the form

$$\begin{cases} \frac{du}{dt} = \gamma f(u,v) \\ \frac{dv}{dt} = \gamma g(u,v) \end{cases} \tag{7}$$

where

$$\begin{cases} f(u,v) = -\frac{|C_u|}{C_u}(h(u) - v) \\ g(u,v) = \frac{|C_u|}{C_v}(u - \nu v), \end{cases} \tag{8}$$

$$h(u) = \hat{i}(u) + u = \begin{cases} m_2 u + (m_2 - m_0) + \epsilon, & \text{if } u < -1 \\ m_0 u + \epsilon, & \text{if } -1 \le u \le E \\ m_1 u + (m_0 - m_1)E + \epsilon, & \text{if } u > E \end{cases} \tag{9}$$

and $m_0 = 1 + G_a/G$, $m_1 = 1 + G_r/G$, $m_2 = 1 + G_l/G$, $\epsilon = I/(G|E_l|)$. The normalized dimensionless circuit is shown in Fig. 4(b) in terms of the three parameters C_u, C_v, ν, and the nonlinearity $\hat{i}(u)$. The characteristic $h(u)$ defined by (9) is sketched in Fig. 5. We will see that to obtain Turing patterns from this circuit, we must have $C_u < 0$ and $C_v > 0$. An equivalent circuit that uses only two identical positive

[7] This normalization is equivalent to the unnormalized form upon choosing $G = 1$, $C_1 = C_u$, $C_2 = C_v$, $|E_l| = 1$, and $E_r = E$. Without loss of generality and following standard analysis of Turing patterns [6], γ will be assumed positive.

capacitors is shown in Fig. 4(c). Its equivalence is verified in the Appendix. To avoid clutter, we will denote the normalized time t/RC_0 by t.

The symbol γ is chosen to coincide with the notation used in [6] and is distinct from that used in the standard normalization (see the Appendix). To summarize, the standard normalization of the reduced Chua's circuit makes use of the parameters α, m_0, m_1, m_2, ϵ, ν, with $m_1 = m_2$, while in the new one α is replaced by $\gamma = 1/|C_u|$ and, in addition, two extra parameters C_v (which was previously included in α) and E are introduced. Moreover, we allow $m_1 \neq m_2$ so that $h(u)$ need not be symmetric with respect to some point on the curve.

B. Equilibrium Point of the Isolated Cell

The reduced Chua's circuit is a nonlinear autonomous system. **The first assumption we make concerning the parameters of the isolated cell is that it has only one equilibrium point and it is stable.**[8]

The equilibrium points of the reduced Chua's circuit in Fig. 4(b) are the dc solutions of the resistive part of the cell obtained by open circuiting the two capacitors. Assuming the same parameters as in [2], namely $\nu = 2$ $(R = 1, R_0 = 1)$, $m_0 = -1$, $m_1 = m_2 = 0.1$, $\epsilon = 2$, and $E = 1$, the v-i curve $\hat{i}(u)$ of the nonlinear resistor and the load line corresponding to the two linear resistors in series; i.e., a 2 Ω resistor, are shown in Fig. 6(a). The intersection Q gives the dc operating point at $U_0 = 2.25$ V. The voltage V_0 across capacitor C_v in Fig. 4(b) is just the voltage across the voltage divider; i.e., $V_0 = \frac{1}{2}(2.25) = 1.125$. Hence, there is a unique equilibrium point located at $(U_0, V_0) = (2.25, 1.125)$ This equilibrium point could of course be calculated directly by solving the following equilibrium equation obtained from (7), as shown graphically in Fig. 6(b)

$$\begin{cases} h(u) - v = 0 \\ -u + \nu v = 0. \end{cases} \tag{10}$$

Stability of the Equilibrium Point: Let us investigate first the local stability of the equilibrium point of an isolated cell. We will assume there is only one equilibrium point (in this case, on the rightmost segment of the nonlinear characteristic). The stability problem is a linear one and the linear(ized) system around the equilibrium point (U_0, V_0) will be asymptotically stable if the characteristic polynomial of the linear state equations

$$\begin{cases} \frac{du}{dt} = \gamma(f_u u + f_v v) \\ \frac{dv}{dt} = \gamma(g_u u + g_v v) \end{cases} \tag{11}$$

has both of its roots in the open left hand plane, where $f_u = \frac{\partial f}{\partial u}\big|_{U_0,V_0}$, $f_v = \frac{\partial f}{\partial v}\big|_{U_0,V_0}$, $g_u = \frac{\partial g}{\partial u}\big|_{U_0,V_0}$, $g_v = \frac{\partial g}{\partial v}\big|_{U_0,V_0}$ are the elements of the Jacobian matrix of $f(u, v)$ and $g(u, v)$.

[8]Patterns in two-grid coupled CNNs can be obtained using unstable cells too. However, in this paper, the term *Turing pattern* refers only to patterns produced in CNNs made of stable isolated cells; the distinguishing feature is that even though the equilibrium point of the isolated cells is stable, when they are coupled through the two resistive grids, this equilibrium point, which corresponds to a homogeneous pattern, becomes unstable, and a nonuniform pattern corresponding to another equilibrium point emerges.

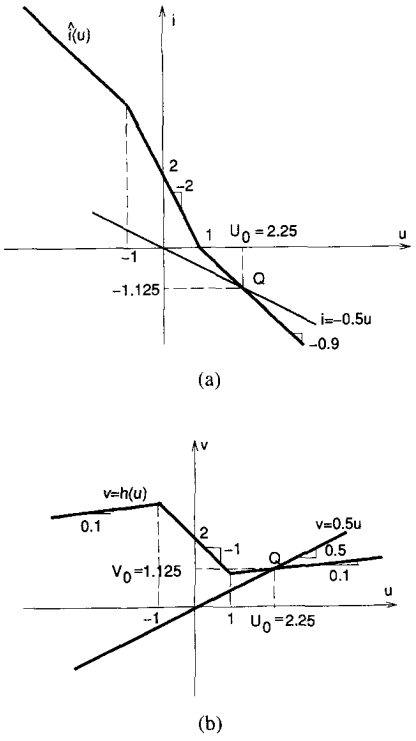

Fig. 6. (a) Graphical construction for determination of equilibrium point using load line method and composition of characteristics. Q: operating point, $\hat{i}(u)$: characteristic of Chua's diode in Fig. 4(b), $i = -0.5u$: load line. (b) Graphical solution of system (10).

The elements f_u, f_v, g_u, g_v have, for the equilibrium point (U_0, V_0) on the right branch of the characteristic[9], the values: $f_u = -\frac{|C_u|}{C_u} m_1$, $f_v = \frac{|C_u|}{C_u}$, $g_u = \frac{|C_u|}{C_v}$, $g_v = -\frac{|C_u|}{C_v}\nu$. The corresponding linear(ized) equations are

$$\begin{cases} \frac{du}{dt} = \gamma\left[-\frac{|C_u|}{C_u} m_1 u + \frac{|C_u|}{C_u} v\right] \\ \frac{dv}{dt} = \gamma\left[\frac{|C_u|}{C_v} u - \nu\left(\frac{|C_u|}{C_v}\right) v\right]. \end{cases} \tag{12}$$

In terms of f_u, f_v, g_u, g_v the characteristic polynomial is

$$\det\begin{vmatrix} \lambda - f_u & -f_v \\ -g_u & \lambda - g_v \end{vmatrix} = 0; \tag{13}$$

i.e.,

$$\lambda^2 - (f_u + g_v)\lambda + f_u g_v - f_v g_u = 0 \tag{14}$$

and has the roots

$$\lambda_{1,2} = 0.5\left(f_u + g_v \pm \sqrt{(f_u - g_v)^2 + 4 f_v g_u}\right). \tag{15}$$

To have both roots strictly in the left hand plane, the following conditions should be fulfilled simultaneously

$$\begin{cases} f_u + g_v < 0 \\ f_u g_v - f_v g_u > 0. \end{cases} \tag{16}$$

The first condition ensures that, for complex roots, their real part is negative, and the second one refers to real roots for which the greatest value should be negative. It is obvious that the values $f_u = 0.1$, $f_v = -1$, $g_u = 0.1$, $g_v =$

[9]When the equilibrium point is on the middle part of the piecewise-linear characteristic, m_1 should be replaced by m_0.

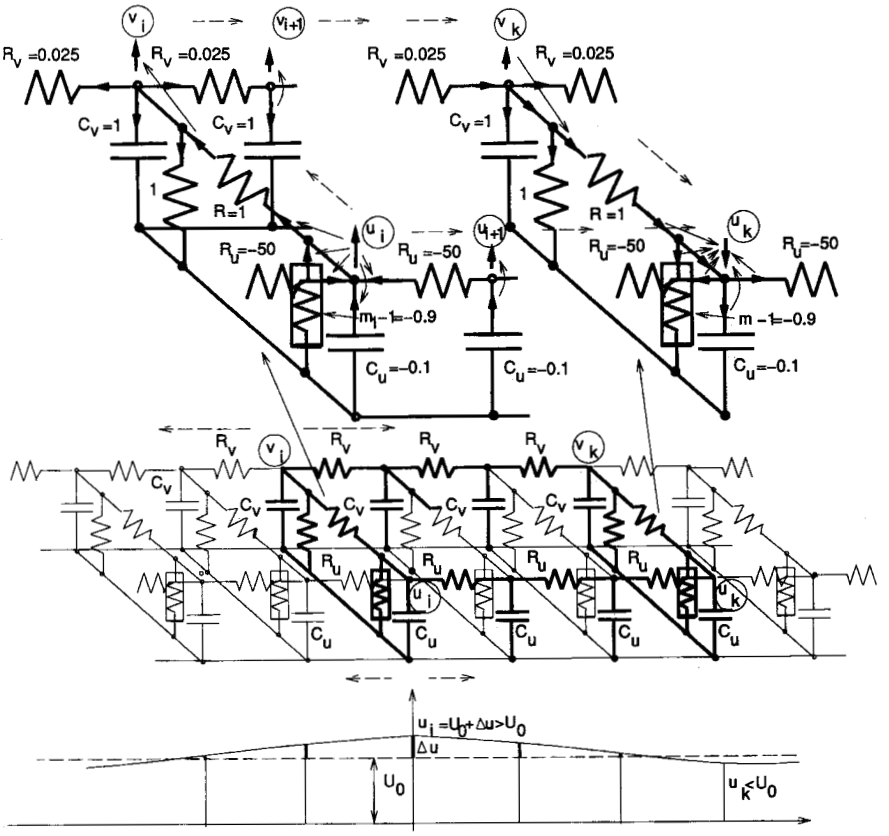

Fig. 7. 1–D two-grid coupled CNN.

-0.2 correspond to a stable cell: the eigenvalues are $\lambda_{1,2} = \frac{-1 \pm j\sqrt{31}}{20}$. The above values correspond to $C_u = -0.1$ ($\gamma = 10$), $C_v = 1$, and $\nu = 2$. Observe that the position of the equilibrium point does not depend on $C_u(\gamma)$ and C_v, but its stability obviously *does* depend on the capacitor values through g_u and g_v.

Observation: By choosing $\epsilon = 0$ and appropriate values for the parameters (e.g., $\nu = 2$, $m_0 = 0.1$, $m_1 = m_2 = -1$, $E = 1$) there is a unique stable equilibrium point at the origin ($U_0 = V_0 = 0$).

III. Coupling the Cells: The Two-Grid Coupled CNN

In this paper, the CNN is made of the above second-order Chua's circuit as basic cells and has the structure shown in Fig. 2. Since the resulting network is much more complex than a simple cell, much more complex dynamics as well as a diversity of equilibrium points can be expected. In fact, the network is described by a system of 2 MN nonlinear ordinary differential equations. Observe that the array will still have an equilibrium point having (U_0, V_0) for all cells because all node voltages on each grid are then identical, and hence, the currents through the resistors of the grids are zero. In this case, the cells will behave as if they were uncoupled. However, by the usual definition of a Turing pattern, **this homogeneous equilibrium point (regarded as an equilibrium for the CNN) must become unstable so that the array can evolve to other (stable) equilibria** depending on the boundary and initial conditons. Before making a rigorous analysis of the dynamics of the two-grid coupled CNN, let us consider an intuitive explanation directly related to the famous "reaction-diffusion" mechanism proposed by A. Turing and several general qualitative features of pattern formation.

Intuitive Explanation of Pattern Formation in a 1-D Array: Qualitative explanations, when possible, could be useful for intuitive understanding of a phenomenon and also for mathematical modeling, when its governing physical laws are not (completely) known. However, we should warn the reader that the same system may exhibit qualitatively different behaviors for other values of the parameters.

Consider the 1-D CNN shown in Fig. 7 where C_u and R_u are negative and the diffusion coefficients $D_u = 1/R_u C_u$ and $D_v = 1/R_v C_v$ satisfy the relation $D_v > D_u > 0$. Suppose that at the beginning all cells are operating in their (individual) equilibrium point (U_0, V_0), which is also an equilibrium point for the whole CNN as we already observed above. No currents flow through the grid resistances in this case. The essence of the following discussion is to suggest how, due to a small perturbation and to different "diffusion" coefficients, a differentiated spatial behavior occurs. We will focus on cells i and k and the *RC* coupling network represented with thick lines in Fig. 7.

First Feature—Local Activation: Suppose that a local perturbation causes a small increase of the voltage from $u_i = U_0$ to $u_i = U_0 + \Delta u$ across the capacitor C_u connected to the u_ith node as shown by a vertical arrow in the left-upper part of Fig. 7. Now, remember that all elements connected to this node except the cell's transversal resistor R (i.e., R_u and C_u) are negative or operate on a negative-slope

piecewise-linear domain (Chua's diode). The above increase will have *transversal* effects on the value of v_i and *longitudinal* effects, through the R_uC_u couplings on the values of u_{i-1}, $u_{i-2}\ldots$ and u_{i+1}, $u_{i+2}\cdots u_k\ldots$. First, an increase of the current through the transversal resistor R of the ith cell will inject some part of this current into capacitor C_v charging it, thereby increasing the voltage v_i of the opposite node as depicted by arrows on the left cell i in the upper part of Fig. 7. The longitudinal effect of the initial perturbation will be to increase the current through the u-grid resistors with the direction shown in the figure (since $R_u < 0$) and, consequently, to increase the voltages of the neighboring u-nodes (since $C_u < 0$). Thus, u_i behaves as a *local "activator"* for both the u and v neighboring variables.

Second Feature—Distant Inhibition: The emergence of a pattern would not be possible if the "diffusion" coefficients were equal. At this stage of our qualitative description, we show the key role in pattern formation of the unbalance of the "diffusion" coefficients D_u and D_v; i.e., of the fact that u "diffuses" more slowly than v. Roughly speaking, this unbalance can be seen as a difference in the "speeds" with which a perturbation is sensed by distant nodes through the u-grid compared with the v-grid. First, observe that, due to the positive values of the elements connected to the v-nodes, an increase of the voltage will induce an *increase* of the neighboring v-node voltages as depicted by arrows in the figure. We now focus on the kth cell further to the right. For the values $C_u = -0.1$, $R_u = -50$, $C_v = 1$, and $R_v = 0.025$, the time constants of the R_uC_u circuits are 200 times greater than that of the R_vC_v circuits.[10] Thus, the node v_k will sense the perturbation from node v_i earlier than the node u_k senses the perturbation from the node u_i. Consequently, *the behavior of u_k will be determined by v_k rather than by u_i* as follows (see Fig. 7); an increase of v_k will induce an increase in the current through the R resistor of the kth cell with the direction indicated in the figure. Due to the negative values of the elements connected to the node u_k, the currents induced by the increase of v_k, with the direction shown in the figure, will cause u_k to decrease. We remark that v_k has an "inhibiting" effect on u_k. We have thus a *long-range "inhibition" effect* exerted by the v_i voltage, through v_k, on the voltage u_k. Also observe that, if we focus on the kth cell, the voltage v_k has a local "inhibitory" effect on the voltage u_k. Summarizing, the mechanism of pattern formation is the result of the interaction of the variables u and v, which behave as activators and inhibitors, respectively. Similar considerations can be made for a 2-D array.

In the above explanation, we have made use of the rather unusual terms of "activation" and "inhibition" to make a connection with the original mechanism of reaction-diffusion proposed by A. Turing. Since the reader is probably unfamiliar with the terminology used by chemists on Turing patterns, it might be more instructive to present first a "circuit" explanation and then to briefly review the principle used by Turing. A useful "dictionary" for this translation is to make the dynamics of a single cell correspond to what the chemists call a "reaction" between u (activator) and v (inhibitor) and to make the dynamics of the whole array correspond to "reaction" plus "diffusion" of u and v.

Qualitative Description of Turing's Reaction-Diffusion Principle: In his famous 1952 paper *"The chemical basis of morphogenesis"*[11] Alan Turing proposed to model pattern development in biological arrays of cells by an interaction of chemicals called *morphogens*. The simplest model uses two morphogens (whose *concentrations* are the state variables of the cells) called an activator and an inhibitor. The interaction between these morphogens has two aspects: reaction and diffusion. Locally, the activator reacts with itself in an excitatory (auto-catalytic) manner and also activates the inhibitor; the inhibitor reacts with itself in an inhibitory manner and also inhibits ("consumes") the activator.[12] The reaction alone is not able to produce patterns. The mechanism that will provide the long-range inhibition is the differentiated diffusion behavior of the morphogens; the activator must have a smaller diffusion rate than the inhibitor. Thus, at long-range, the inhibitor not only will inhibit the activator's tendency to increase but also will cause it to decrease (auto-catalytically as well). The initial decrease will determine a further decrease and so on. Thus, at long-range, the activator's concentrations will decrease.

Terminology and Basic Principle of Pattern Formation: From the above short explanations, it is apparent that, roughly speaking, the interactions between the variables involved in a dynamics leading to a pattern may be excitatory (activating) and/or inhibitory. Such interactions may take place between local variables and between local and distant (similar or different) ones. Thus, since we refer to initially homogeneous systems, the mechanism of pattern formation should provide the following two features:

—breakdown of the homogeneous steady-state symmetry and

—differentiated behavior in space.

The above conditions are realized through local activation (symmetry breakdown) and long range inhibition (differentiated spatial behavior).

Several qualitative features of pattern formation are given in the following with reference to the qualitative behavior of the above-presented 1-D two-grid coupled CNN that has all ingredients of a pattern-producing mechanism:

- Tendency toward instability of the homogeneous state (the homogeneous equilibrium state of the array is unstable).
- The existence of certain specific interactions between local state variables and between local ones and distant ones. The above interactions could be highly nonlinear, but for restricted domains, some of them should be locally excitatory and inhibitory at long-range. (Choosing a piecewise nonlinear characteristic in the reduced Chua's circuit makes things more tractable.)

[10] In fact, there will be loading effects exerted by the resistive parts of the cells, but since the resistances in parallel to the capacitors have approximatively equal absolute values (1 and −0.9), the above statement still remains qualitatively true.

[11] Considered by theoretical biologists as the most important paper of the century in this area. Turing is also considered the father of computer science through his invention of the *Turing Machine*.

[12] Turing pattern may appear if the local influence the two morphogens have upon each other is opposite to the above as well.

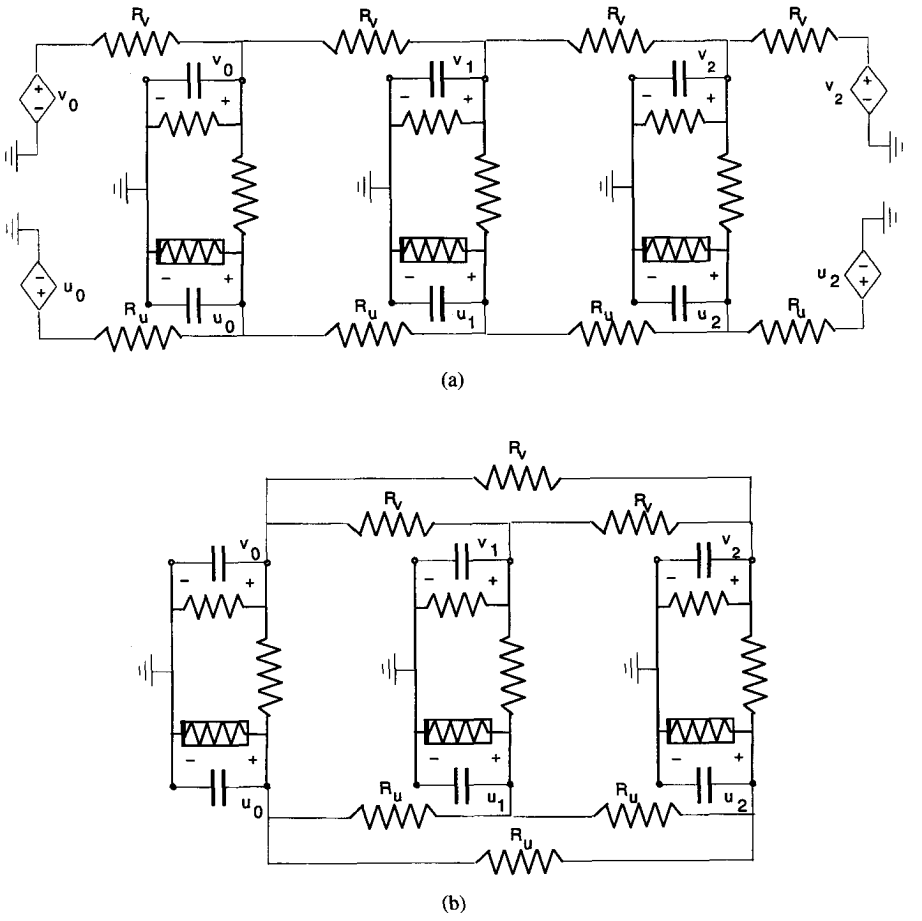

Fig. 8. Three-cell CNN with zero-flux (a) and periodic, (b) boundary conditions.

- Dynamical character. The cells of the CNN contain capacitors; i.e., conservative elements.
- The existence of a nonlinear mechanism that influences the final pattern and also bounds the values of the state variables. In our case, the nonlinearity of the piecewise linear resistor plays this role.
- The dependence of the pattern on the initial and boundary conditions, as well as on the shape and geometrical dimensions of the domain. Pattern development is possible only for a restricted domain of the parameters governing the phenomena.

IV. Initial and Boundary Conditions; Equilibrium Points

Initial and Boundary Conditions: Let us return to the CNN made of second-order Chua's circuits. It will be described by a set of 2MN state equations (which are derived in Part II of this paper) as there are no capacitor loops, each cell is second order and there are MN cells. To solve such a system of ordinary nonlinear differential equations, the initial conditions; i.e., the initial values of the voltages of the capacitors should be known. The CNN "processes" the initial condition and may produce a pattern. Random initial conditions are appropriate to model a physical realization if no other mechanism for imposing initial conditions exists. We discuss in the following the boundary conditions. The main observations are that using the same number of cells and the same M and N, (slightly) different CNNs can be obtained depending on the way the edge cells are connected; i.e., on the boundary conditions.

Let us imagine a cell on one side of a rectangular array. If it is not a corner cell, each capacitor is connected, through resistors, with only 3 neighbor cells (2, for corner cells). For the other end of the fourth resistor (outside of the boundary) one of the following possibilities will be considered:

1) The *zero-flux*[13] boundary conditions correspond to the case when the free ends of all coupling (grid) resistors are not connected (i.e., these resistors can be deleted). In this case, the value of the boundary conditions are precisely the values of the voltages of the boundary cells of the array. (This is as if each edge cell is connected to some external cell consisting of a controlled voltage source that mimics its behavior.) The boundary conditions are, in the 2-D case:[14] $u(-1,j,t) = u(0,j,t)$; $u(i,-1,t) = u(i,0,t)$; $u(M,j,t) = u(M-1,j,t)$; $u(i,N,t) = u(i,N-1,t)$, and similarly for the v variable. For example, a 1-D three-cell CNN with zero-flux boundary conditions is shown in Fig. 8(a).

[13]The term comes from the continuous reaction-diffusion case when the zero-flux boundary condition reads $(\mathbf{n}\cdot\nabla)\mathbf{u} = 0$ for (x,y) on the boundary of the reaction-diffusion domain ($\mathbf{n}$ is the vector normal to the boundary) which implies that the external medium does not influence the system in any way.

[14]The cells are numbered from zero to $M-1$ and $N-1$, respectively.

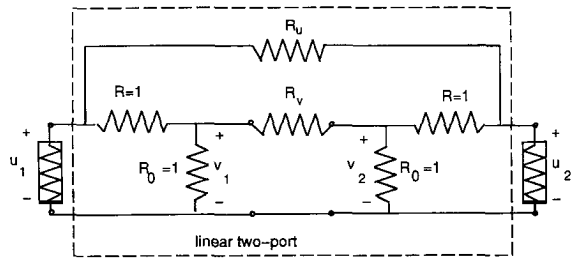

(a)

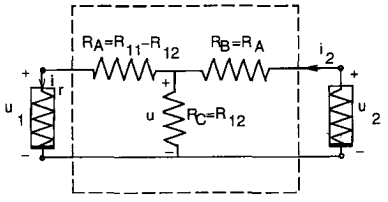

(b)

Fig. 9. (a) Two-cell CNN viewed as a linear two-port loaded with two nonlinear resistors. (b) Equivalent circuit.

2) *Periodic boundaries:* This situation corresponds to a ring (in the 1-D case) or a torus (in the 2-D case) when the cells from the opposite ends of each row and column are connected through a common resistor of the same value as that of the array resistors. Thus, in fact, there are no boundaries. The corresponding "boundary" relations are $u(-1,j,t) = u(M-1,j,t)$; $u(0,j,t) = u(M,j,t)$; $u(i,-1,t) = u(i,N-1,t)$; $u(i,0,t) = u(i,N,t)$, and similarly for v. The same 1-D three-cell CNN for the periodic boundary conditions case is shown in Fig. 8(b).

Other types of boundary conditions are also possible. In this paper, we describe only the example of applying a side-wall forcing [2]; the boundary cells are independent voltage sources, and thus, the CNN is no longer autonomous for time-varying sources.

Summarizing, to solve the system of differential state equations describing the CNN, one needs $2MN$ initial conditions $(i = 0,1,\ldots,M-1,\ j = 0,1,\ldots,N-1)$

$$u(i,j,0), \quad v(i,j,0) \tag{17}$$

for the "temporal" part and $4(M+N)$ boundary conditions $(i = 0,1,\ldots,M-1,\ j = 0,1,\ldots,N-1)$ for all values of $t \in [0,\infty)$

$$\begin{matrix} u(-1,j,t) & u(i,-1,t) & v(-1,j,t) & v(i,-1,t) \\ u(M,j,t) & u(i,N,t) & v(M,j,t) & v(i,N,t) \end{matrix} \tag{18}$$

for the "spatial" part.

How Multiple Equilibria Are Born: The nonlinear equations of the two-grid coupled CNN should have at least another equilibrium point different from that corresponding to (U_0, V_0) and which is stable. In fact, depending on the parameters of the cells, the diffusion constants and the dimensions of the array, there may be many stable equilibria, each one corresponding to a different pattern. Of course, the system may have unstable equilibrum points as well, the already discussed homogeneous equilibrium point being one of them. Which equilibrium point will the CNN converge to depends on which basin of attraction does the initial condition lie. To illustrate the complexity of the equilibrium point problem, let us consider the simplest possible CNN made of only two cells, subject to a zero-flux or a periodic boundary condition, respectively. We will show that even in such simple cases many equilibrium points are possible. The two-cell CNN configuration is shown in Fig. 9(a) and corresponds to zero-flux conditions; both cells in this case are edge cells, and no other connections are necessary (the currents through the boundary resistors connecting the controlled source to the edge cells are zero, and those resistors can be deleted). For *periodic* boundary conditions, the opposite cells should be linked through resistors of the same values to that of the grids as shown in Fig. 8(b). Observe that in this case there will be two extra resistors linking the corresponding nodes so that (only in the case of two-cell CNNs) the ring configuration differs from the zero-flux only by the values of the resistors R_u and R_v in Fig. 9(a); for periodic boundary conditions, the resistors R_u and R_v should be replaced by resistors having the values $0.5R_u$ and $0.5R_v$, respectively. In view of this observation, only one set of calculations need be made. Observe that the circuit in Fig. 9(a) (where the cells have been numbered with 1 and 2) can be viewed as a linear two-port loaded with two nonlinear resistors. The two-port is reciprocal and symmetric and is described by a resistance matrix

$$\mathbf{R} = \begin{bmatrix} R_{11} & R_{12} \\ R_{21} & R_{22} \end{bmatrix} \tag{19}$$

whose elements satisfy $R_{11} = R_{22}$ and $R_{12} = R_{21}$ and are determined by the following relations in terms of the grid and linear resistances of the cells:

$$\begin{aligned} R_{11} &= \frac{2R_u(1+R_v)}{4(1+R_v)+R_u(2+R_v)} \\ R_{12} &= \frac{R_u+4(R_v+1)}{4(1+R_v)+R_u(2+R_v)}. \end{aligned} \tag{20}$$

Moreover, using standard techniques from circuit theory (the $\Delta - Y$ equivalence) the linear two-port can be transformed into a (symmetric) T configuration as shown in Fig. 9(b). Assuming $G_u = \frac{1}{R_u} = -0.02$ and $G_v = \frac{1}{R_v} = 40$, the following values are obtained: $R_A = R_B = 1.055$ and $R_C = 0.451$.

Now it is an easy task to obtain all the equilibrium points of the CNN. The successive geometric constructions are presented in Fig. 10 as follows: the equivalent characteristic of the left nonlinear resistor in series with R_A is presented in Fig. 10(a), the characteristic of the resulting nonlinear resistor in parallel with the linear resistor R_C is sketched in Fig. 10(b), and the characteristic of the last one in series with the linear resistor $R_B = R_A$ is shown in Fig. 10(c). Assuming the same values for the grid conductances as above, the equivalent nonlinear resistor "seen" at the right port is described by the following voltage–current relations:

$$\begin{cases} i_2 = 1.005u_2 - 1.14 & u_2 \le 3.35 \\ i_2 = 0.726u_2 - 0.202 & 3.36 \le u_2 \le 13.36 \\ i_2 = 1.005u_2 - 3.931 & u_2 \ge 13.36. \end{cases} \tag{21}$$

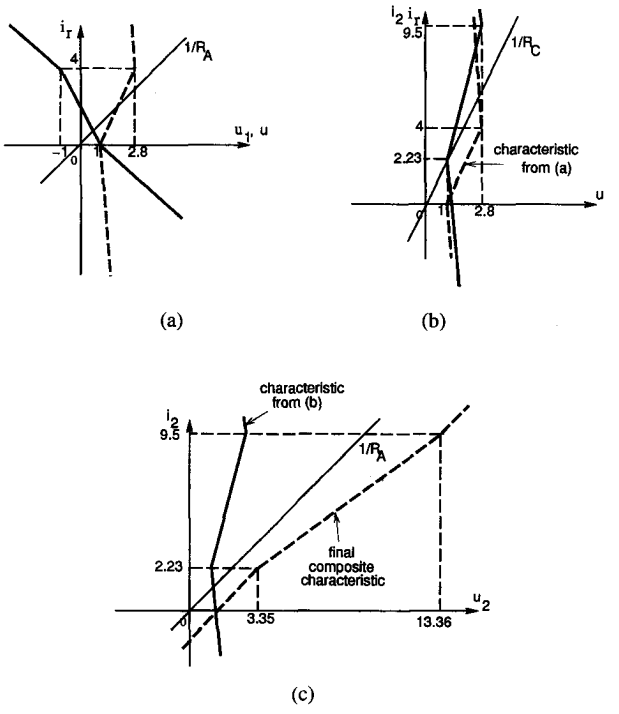

Fig. 10. Graphical constructions for obtaining the equivalent voltage–current nonlinear characteristic of port 2. The composite characteristics are shown with broken line.

At this stage, the circuit consists of a parallel connection of two nonlinear resistors: Chua's diode of the second cell and the equivalent nonlinear resistor; thus, the problem of finding the equilibrium points for the CNN is straightforward. The geometrical "load line" [11] construction is shown in Fig. 11. Observe that for the chosen numerical values there are five operating points corresponding to the following u-voltages: $u_2 = -18.6$, $u_2 = 0.86$, $u_2 = 2.25$, $u_2 = 4.0$, and $u_2 = 28.6$. Due to the symmetry of the CNN, the same values are valid for the voltage u_1 of the first cell. Thus, the five equilibrium points of the CNN in terms of the u-voltages are: $(u_1, u_2) = (28.9, -18.6)$, $(u_1, u_2) = (4.0, 0.86)$, $(u_1, u_2) = (2.25, 2.25)$, $(u_1, u_2) = (0.86, 4.0)$, $(u_1, u_2) = (-18.6, 28.9)$. In the first and the last case, the equilibrium points lie on the rightmost, and respectively, leftmost parts of the piecewise-linear characteristics of Chua's diode. In the second and fourth case, the equilibrium point lies on the rightmost segment of the nonlinear resistors for one cell and on the middle segment for the other cell. Finally, the third operating point corresponds to the cells operating both on the middle characteristic of the nonlinear resistors. This is the spatially homogeneous equilibrium point identical to (U_0, V_0) obtained for the isolated

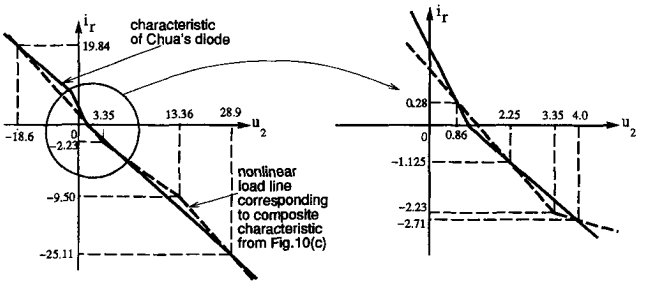

Fig. 11. Load line construction for the determination of the equilibrium points of the two-cell CNN.

cell. In this case, the currents through the resistive grids are zero and, by definition, this spatially homogeneous equilibrium point should be unstable to have Turing patterns.

Obviously, the above results[15] and geometric constructions as well as the stability of the equilibrium points depend on the values of the cell parameters and the grid resistances as well. However, this simple example shows that even in the case of a two-cell CNN, already five equilibrium points are possible. We conjecture that the number of equilibrium points increases exponentially with the number of cells.

APPENDIX
BRIEF REVIEW OF CHUA'S CIRCUIT

In the following, we first briefly review the third-order Chua's circuit (Fig. 3) where the inductor is present; i.e., it is *not* short circuited. The state equations describing this circuit are

$$\begin{cases} \frac{dv_1}{dt} = \frac{1}{C_1}[G(v_2 - v_1) - i(v_1)] \\ \frac{dv_2}{dt} = \frac{1}{C_2}[G(v_1 - v_2) + i_3] \\ \frac{di_3}{dt} = -\frac{1}{L}(v_2 + R_0 i_3) \end{cases} \tag{22}$$

where

$$i = i(v_1) = \begin{cases} G_l v_1 + (G_a - G_l)E_l + I & \text{if } v_1 < E_l \\ G_a v_1 + I & \text{if } E_l \le v_1 \le E_r \\ G_r v_1 + (G_a - G_r)E_r + I & \text{if } v_1 > E \end{cases} \tag{23}$$

and $G = 1/R$. Using the notations

$$G'_a = G + G_a, \quad G'_r = G + G_r, \quad G'_l = G + G_l, \tag{24}$$

the state equations of Chua's circuit become (see (25) at the bottom of this page).

[15] For periodic boundary conditions; i.e., ring configuration R_u and R_v should be replaced by $0.5R_u$ and $0.5R_v$, respectively.

$$\begin{cases} \frac{dv_1}{dt} = -\frac{G}{C_1}v_1 - \frac{1}{C_1}i(v_1) + \frac{G}{C_1}v_2 = \begin{cases} -\frac{G'_l}{C_1}v_1 + \frac{G}{C_1}v_2 - \left(\frac{G'_a - G'_l}{C_1}\right)E_l - \frac{I}{C_1}, & \text{if } v_1 < E_l \\ -\frac{G'_a}{C_1}v_1 + \frac{G}{C_1}v_2 - \frac{I}{C_1}, & \text{if } E_l \le v_1 \le E_r \\ -\frac{G'_r}{C_1}v_1 + \frac{G}{C_1}v_2 - \left(\frac{G'_a - G'_r}{C_1}\right)E_r - \frac{I}{C_1}, & \text{if } v_1 > E_r \end{cases} \\ \frac{dv_2}{dt} = \frac{G}{C_2}v_1 - \frac{G}{C_2}v_2 + \frac{1}{C_2}i_3 \\ \frac{di_3}{dt} = -\frac{1}{L}v_2 - \frac{R_0}{L}i_3 \end{cases} \tag{25}$$

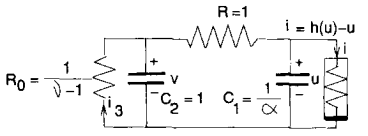

Fig. 12. Standard normalization of the reduced Chua's circuit.

Standard Normalization of Chua's Circuit: The usual way of normalizing Chua's circuit for the particular case $-E_l = E_r = E = 1$, $G_l = G_r = G_b$ is based on the relations $\tau = \frac{t}{RC_2}$, $u = \frac{v_1}{E}$, $v = \frac{v_2}{E}$, $w = \frac{Ri_3}{E}$, $\alpha = \frac{C_2}{C_1}$, $\beta = \frac{R^2C_2}{L}$, $\gamma = \frac{R_0RC_2}{L}$, $\epsilon = \frac{I}{GE}$, $m_0 = \frac{G_a}{G} + 1$, $m_1 = m_2 = \frac{G_b}{G} + 1$, and leads to the following dimensionless equations

$$\begin{cases} \frac{du}{d\tau} = \alpha(-h(u) + v) \\ \frac{dv}{d\tau} = u - v + w \\ \frac{dw}{d\tau} = -\beta v - \gamma u \end{cases} \tag{26}$$

where $h(u) = u + \hat{i}(u) = m_1 u + 0.5(m_0 - m_1)(|u + 1| - |u - 1|) + \epsilon$

Standard Normalization of the Reduced Chua's Circuit: The state equation (4) of the reduced Chua's circuit when the inductor is short circuited (Fig. 3(a)) can be normalized using the same relations as above and defining $\nu = 1 + \frac{G_0}{G}$ [2]. These equations are

$$\begin{cases} \frac{du}{d\tau} = \alpha(-h(u) + v) \\ \frac{dv}{d\tau} = u - \nu v. \end{cases} \tag{27}$$

The dimensionless circuit is shown in Fig. 12. The reduced Chua's circuit can also be obtained from the original dimensionless third-order Chua's circuit by using a limiting argument: $\beta \to \infty$; $\gamma \to \infty$; $\frac{\beta}{\gamma}$ = finite; $\nu = 1 + \frac{\beta}{\gamma}$; $w = -\frac{\beta}{\gamma}v$.

Equivalent Normalized Reduced Chua's Circuit: The reduced Chua's circuit normalized by means of the relations (6) can be represented in an equivalent form making use of two identical capacitors directly related to the parameter γ used in standard theory of Turing patterns [6]. The circuit is shown in Fig. 4(c), and is described by the following parameters: $\hat{G}_1 = \frac{|C_u|}{C_u}$, $\hat{G}_2 = \nu\frac{|C_u|}{C_v} - \frac{|C_u|}{C_u}$, $\hat{G}_3 = \frac{|C_u|}{C_v} - \frac{|C_u|}{C_u}$, $\hat{i}_R = \hat{g}(\hat{v}_R) = \frac{|C_u|}{C_u}[h(\hat{v}_1) - \hat{v}_1]$.

REFERENCES

[1] R. Madan, *Chua's Circuit: A Paradigm for Chaos.* Singapore: World Scientific, 1993.

[2] A. Pérez-Muñuzuri, V. Pérez-Muñuzuri, M. Gómez-Gesteira, and L. O. Chua, "Spatio-temporal structures in discretely-coupled arrays of nonlinear circuits: A review," *Int. J. Bifurc. and Chaos*, vol. 5, no. 1, Feb. 1995.

[3] H. Bénard, "Les tourbillons cellulaires dans une nappe liquide," *Rev. Gén. Sciences Pure Appl.*, vol. 11, pp. 1261–1271, 1309–1328, 1900.

[4] E. L. Koschnmieder, *Benard Cells and Taylor Vortices.* Cambridge, MA: Cambridge Univ. Press, 1993.

[5] A. M. Turing, "The chemical basis of morphogenesis," *Phil. Trans. Roy. Soc. Lond.*, B 237, pp. 37–72, 1952.

[6] J. D. Murray, *Mathematical Biology.* Berlin: Springer-Verlag, 1989.

[7] L. O. Chua and L. Yang, "Cellular neural networks: Theory," *IEEE Trans. Circuits Syst.*, vol. 35, pp. 1257–1272, Oct. 1988.

[8] ——, "Cellular neural networks: Applications," *IEEE Trans. Circuits Syst.*, vol. 35, pp. 1273–1290, Oct. 1988.

[9] T. Roska and J. Vanderwalle, Eds. *Cellular Neural Networks.* New York: Wiley, 1993.

[10] A. L. Zheleznyak and L. O. Chua, "Coexistance of low-and high-dimensional spatio-temporal chaos is a chain of dissipateively coupled Chua's circuits," *Int. J. Bifurc. and Chaos*, vol. 4, no. 3, pp. 639–674, 1994.

[11] L. O. Chua, *Introduction to Nonlinear Network Theory.* New York: McGraw Hill, 1969.

[12] K. R. Crounse and L. O. Chua, "Methods for image processing and pattern formation in cellular neural networks: A tutorial," *IEEE Trans. Circuits Syst.*, vol. 42, no. 10, pp. 583–601, this issue.

[13] K. R. Crounse, P. Thiran, G. Setti, and L. O. Chua, "Characterization and dynamics of pattern formation in cellular neural networks," to be published in *Int. J. Bifurc. and Chaos*, vol. 6.

Liviu Goraş (M'91) was born in Iasi, Romania on October 20, 1948. He received the Diploma and Ph.D. degree in electrical engineering from the Technical University "Gh. Asachi", Iasi, Romania in 1971 and 1978, respectively.

He was successively Assistant, Lecturer, Associate Professor, and since 1994 , he has been a Professor with the Faculty of Electronics and Telecommunications, TU Iasi. His main research interests, reflected by his published papers, are nonlinear circuit and system theory and signal theory. He is the author of the book *Signal, Circuits and Systems* written in Romanian. From September 1994 to May 1995, he was on leave, as a senior Fulbright scholar, at the Department of Electrical Engineering and Computer Sciences, University of California at Berkeley.

Leon O. Chua (S'60–M'62–SM'70–F'74), for a photograph and biography, see this issue, p. 558.

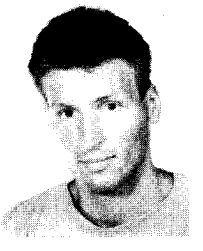

Domine M. W. Leenaerts (M'94) received the Ir. and Ph.D. degree in electrical engineering from the Technical University Eindhoven, The Netherlands in 1987 and 1992, respectively.

He is currently an Assistant Professor at the same university. In 1995, he has been a Visiting Scholar at the Department of Electrical Engineering and Computer Sciences and the Electronics Research Laboratory of UC, Berkeley. His main research areas in electronic circuits and systems have been nonlinear dynamics system theory, piecewise linear theory, and (the automation of) circuit design, and he has published several papers in these areas.